Ab Initio Calculation of Phase Diagrams of Oxides

M. Yu. Lavrentiev,[†,‡] N. L. Allan,[*,‡] G. D. Barrera,[§] and J. A. Purton[⊥]

School of Chemistry, University of Bristol, Cantock's Close, Bristol BS8 1TS, U.K., Departamento de Química, Universidad Nacional de la Patagonia SJB, Ciudad Universitaria, (9005) Comodoro Rivadavia, Argentina, and Central Laboratory of the Research Councils, Daresbury Laboratory, Warrington, Cheshire WA4 4AD, U.K.

Received: November 9, 2000; In Final Form: February 6, 2001

We show how Monte Carlo simulations with the explicit interchange of cations, the semigrand-canonical ensemble and configurational bias techniques, can be used to calculate phase diagrams for oxides, including both solid *and* liquid phases. We illustrate our approach with the system CaO/MgO where our techniques take full account of local structural distortion and clustering due to the large mismatch between the sizes of the two cations. All the characteristic features of the MgO/CaO phase diagram, including the eutectic point and the regions of liquid−solid coexistence, are reproduced.

Introduction

Solid solutions, nonstoichiometry, and phase stability present considerable challenges for theory. Energy differences between different phases can be small and subtle cation ordering effects can be often crucial in determining phase stability and thermodynamic and chemical properties. Oxide solutions in particular are often strongly nonideal. An understanding of nonideal behavior and ordering can also be fundamental for the interpretation of any process involving partitioning of trace elements between two solid phases, or between solid and melt. Approaches such as the Cluster Variation Method (CVM),[1] widely used for metallic alloys, often perform poorly where the species involved are markedly dissimilar, as usually occurs in oxides and minerals. In addition, accurate thermodynamic data for oxide solutions is rare despite the evident importance of such information in areas as diverse as mineralogy and ceramic fabrication and design.

Disorder in *solid* oxides has largely been investigated theoretically via point defect calculations[2] (the dilute limit), or via "supercells",[3] in which a superlattice of defects is introduced, extending throughout the macroscopic crystal. The periodicity is then that of the particular superlattice chosen and convergence toward properties of an isolated defect occurs as the superlattice spacing is increased. These methods are not readily extended to solid solutions, liquid phases, or disordered systems with a *finite* impurity or defect content far from the dilute limit.

We are currently developing a series of new codes and methods to address such problems. A key feature of all of these is the need to sample many different arrangements of ions, allowing for the exchange of ions located at crystallographically inequivalent positions. Any method must also take into account the local environment of each ion and the local structural movements (relaxation), which accompany any exchange of ions and reduce considerably the energy associated with any such interchange. Local effects due to ion association or clustering should not be averaged out. Methods should be readily extendible to incorporate the effects of high pressure or thermal (vibrational) effects. The use of parametrized Hamiltonians (e.g., of Ising type) is increasingly difficult beyond binary or pseudobinary alloys and so we have not resorted to any such approximate scheme.

In this paper we extend earlier work[4,5,6] restricted to solid phases and illustrate our approach using the CaO/MgO system. This presents particular complications due to the large difference in ionic radius[7] between Ca^{2+} (1.00 Å) and Mg^{2+} (0.72 Å). For the first time we now calculate the *entire* phase diagram, including all liquid and solid phases, using new Monte Carlo methods. Our simulations, the determination of the melting points and the extraction of the phase diagram are all discussed in subsequent sections. Results for enthalpies, entropies, and the phase diagram are then presented and compared with experiment. Where possible, results for the solid phase at low T are also compared with those obtained from our new configurationally averaged lattice dynamics technique[5,8] for solid solutions.

Exchange Bias Monte Carlo

The basis for most of the approaches we discuss is the well-known Monte Carlo method but modified as described below. All Monte Carlo calculations use a box-size of 512 ions and 4×10^7 steps, following initial equilibration of 1×10^7 steps. All calculations in this paper are based on an ionic model using two-body potentials to represent short-range forces; we use the interaction potentials of Lewis and Catlow first introduced in their study of the parent oxides[9] and subsequently employed by Ceder et al.[10]

Our starting point is a Monte Carlo simulation (MC) in which there are *no* cation interchanges. Vibrational effects are taken into account by allowing random moves of randomly selected atoms. Both atomic coordinates and cell dimensions are allowed to vary during the simulation. During one step of the MC simulation an atomic coordinate or a lattice parameter is chosen at random and altered by a random amount. To determine whether the change is accepted or rejected, the usual Metropolis algorithm[11,12] is applied. The maximum changes in the atomic

[†] On leave from Institute of Inorganic Chemistry, 630090 Novosibirsk, Russia.
[‡] School of Chemistry.
[§] Departamento de Química.
[⊥] Central Laboratory of the Research Councils.

10.1021/jp004124+ CCC: $20.00
Published on Web 04/10/2001

displacements and the lattice parameters are governed by the variables r_{max} and v_{max}, respectively. The magnitudes of these parameters are adjusted automatically during the equilibration part of the simulation to maintain an acceptance/rejection ratio of approximately 0.3.

In the MC calculations each step thus comprises either an attempted atom movement or a change of size of the simulation box. The MC calculations thus almost always sample only one cation arrangement, the initial configuration, which is chosen at random. Consequently, for CaO/MgO, the calculated variation of ΔH_{mix} varies erratically with composition, and there is a strong dependence on the choice of the initial arrangement. For example, for a 50/50 CaO/MgO mixture, by choosing different cation arrangements, we were able to vary ΔH_{mix} by as much as 40 kJ mol^{-1}, which is much higher than the final value of ΔH_{mix} obtained below. This erratic variation is even more marked than noted previously for MnO/MgO where the size mismatch between the ions is smaller.

We have described elsewhere[13] Monte Carlo Exchange (MCX) simulations in which *both* the atomic configuration *and* the atomic coordinates of all the atoms are changed. In any step, a random choice is made whether to attempt a random exchange between two atoms, a random displacement of an ion, or a random change in the volume of the simulation box. Again, the Metropolis algorithm is used to accept or reject any attempted move.[14] This technique worked well in previous work[6] for the MnO/MgO solid solution but for CaO/MgO, where there is a much larger mismatch between the cation radii, the rate of successful exchanges in MCX simulations is substantially smaller and only ≈3% of the attempted exchanges. Long runs are thus necessary in order to obtain a good sampling of configurations and these are computationally far too expensive. Special methods are thus necessary to increase the rate of successful exchanges.

To speed up the sampling of configurations, we have applied the biased sampling technique, widely used in simulations of molecules with an orientation-dependent interaction potential (orientational bias) and polymer conformations (configurational bias),[12] to the CaO/MgO solid solution. In our exchange-bias Monte Carlo, instead of considering a single trial exchange, a set of trial exchanges is picked at random. One of these is then chosen as explained below. The acceptance rule differs from the standard Monte Carlo (Metropolis) algorithm. Below, we describe the exchange-bias Monte Carlo algorithm in detail and demonstrate that it satisfies the condition of detailed balance.

Suppose an exchange take place between atoms A and B. First, k pairs $\{A^i, B^i, i = 1, .., k\}$ are randomly chosen. We denote the system energy in the initial configuration as U_{old} and the energy of the system after exchange of atoms in the ith pair as U^i_{new}. One of the new configurations is then chosen with probability

$$p_i = \frac{\exp(-\beta(U^i_{new} - U_{old}))}{W_{new}}, \beta = (kT)^{-1} \quad (1)$$

where

$$W_{new} = \sum_{l=1}^{k} \exp(-\beta(U^l_{new} - U_{old})) \quad (2)$$

The chosen configuration i (that after the exchange of the ith pair) with energy $U^i_{new} \equiv U_{new}$ is then the trial configuration. However, the usual acceptance rule cannot be directly applied. Instead, starting from the new configuration, further $k-1$ pairs A^j, B^j, $j = 1, .., k-1$ are chosen. Denoting the energy of the system after exchange of atoms in the jth pair U^j_{old}, we evaluate the expression

$$W_{old} = \exp(-\beta(U_{old} - U_{new})) + \sum_{j=1}^{k-1} \exp(-\beta(U^j_{old} - U_{new})) \quad (3)$$

The flow of old configuration into the new is

$$K(\text{old} \rightarrow \text{new}) = N(\text{old}) p_i acc(\text{old} \rightarrow \text{new}) \quad (4)$$

and the flow in the opposite direction

$$K(\text{new} \rightarrow \text{old}) = N(\text{new}) p_j acc(\text{new} \rightarrow \text{old}) \quad (5)$$

where

$$p_j = \frac{\exp(-\beta(U_{old} - U_{new}))}{W_{old}} \quad (6)$$

Since the flows in both directions must be equal,

$$\frac{acc(\text{old} \rightarrow \text{new})}{acc(\text{new} \rightarrow \text{old})} = \frac{N(\text{new})}{N(\text{old})} \times \frac{p_j}{p_i} \quad (7)$$

and recalling that

$$\frac{N(\text{new})}{N(\text{old})} = \exp(-\beta(U_{new} - U_{old})) \quad (8)$$

we obtain

$$\frac{acc(\text{old} \rightarrow \text{new})}{acc(\text{new} \rightarrow \text{old})} = \exp(-\beta(U_{old} - U_{new})) \frac{W_{new}}{W_{old}} \quad (9)$$

Hence, fulfilling detailed balance, the criterion for the acceptance of the new configuration is

$$acc(\text{old} \rightarrow \text{new}) = \min\left[1, \exp(-\beta(U_{old} - U_{new})) \frac{W_{new}}{W_{old}}\right] \quad (10)$$

Use of the exchange-bias technique allows us to carry out Monte Carlo simulations for CaO/MgO with a successful exchange rate around 25−30%.

Chemical Potential and the Solid−Liquid Transition

Simulations were performed using the semigrand-canonical ensemble[12,15] at temperatures between 2000 and 4000 K and zero pressure monitoring the enthalpy and volume of the system and the chemical potential difference between Ca^{2+} and Mg^{2+} ions. The latter was calculated as previously implemented by us for the determination of the phase diagram of the solid phases of MgO/MnO.[6] In this method one species, B, is converted into another, A, and the resulting potential energy change $\Delta U_{B/A}$ determined. This is related to the change in chemical potential $\Delta m_{B/A}$ by

$$\Delta m_{B/A} = -kT \ln\left\langle \frac{N_B}{N_A + 1} \exp(-\Delta U_{B/A}/kT) \right\rangle \quad (11)$$

Each fifth step (on average) we evaluate the energy associated with the conversion of a randomly chosen Mg^{2+} ion to Ca^{2+}, $\Delta U_{Mg/Ca}$, and as the simulation proceeds, we determine the average value of the right-hand side of eq 11. Note that the

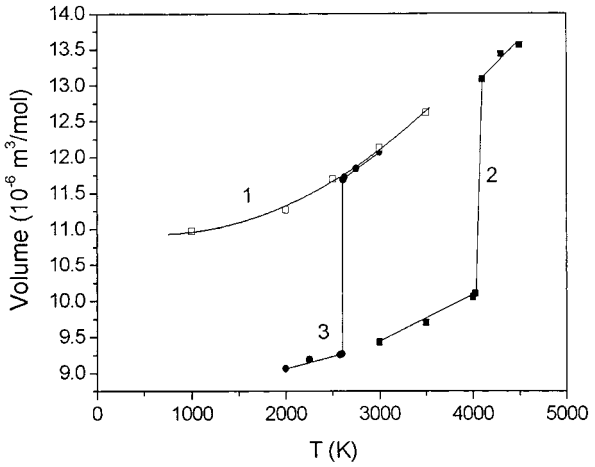

Figure 1. Dependence of the calculated volume with temperature for CaO for different initial configurations: curve 1, liquid phase (□); curve 2, solid phase (■); and curve 3, half-liquid, half-solid simulation box (●).

TABLE 1: Calculated and Experimental Melting Temperatures (K) of MgO and CaO

	calculated	experiment (ref 22)	experiment (ref 23)	experiment (ref 24)
MgO	2870	3098	3125	3098
CaO	2600	2903	2689	3200

change of Mg into Ca is only considered but *not* actually performed—the configuration remains unchanged after evaluating $\Delta U_{Mg/Ca}$. We have checked consistency in that identical results are obtained considering the reverse transformation, i.e., of a randomly chosen Ca^{2+} to a Mg^{2+}.

At $T \approx 3000$ K the system begins to melt. The liquid−solid transition can be seen in the variation of the volume as a function of temperature, with a characteristic jump in volume at the melting point, as shown in Figure 1. It is well-known that it is difficult to locate melting points exactly in Monte Carlo and molecular dynamics simulations if the initial system is homogeneous, because of significant overheating.[16−18] In our Monte Carlo calculations the calculated melting temperature is also too high, if the starting configuration is that appropriate for a solid phase. If instead the simulations start from the liquid phase, the system does not crystallize at low temperatures, but rather freezes into a glasslike state, as illustrated by the *V(T)* dependence also shown in Figure 1. To avoid the hysteresis evident in Figure 1 and establish the melting point, we started the simulation using a simulation box that is half-solid, half-liquid. This strategy has been used successfully in previous molecular dynamics simulations of forsterite,[19] $MgSiO_3$ perovskite[20], and MgO.[21] In our case, we started by performing simulations at a very high temperature (4500 K), where the system is molten for all Ca/Mg concentrations. Then half of the simulation box was filled using a configuration appropriate for the melt, and the other half with perfect solid crystal. In this way the location of the melting point can then be determined to within a few degrees as can also be seen from Figure 1. The calculated melting temperatures T_m for pure MgO and pure CaO are listed in Table 1 together with available experimental data. For both systems, calculated temperatures are 10−15% lower than experiment; but nevertheless it is encouraging that our calculated melting point for CaO is less than that of MgO in agreement with the extensive study of Doman et al.[22] and with the recent tables,[23] rather than with older data.[24] The overall agreement is satisfactory bearing in mind that the potentials were originally fitted to reproduce a range of solid-state properties in the static limit.[9]

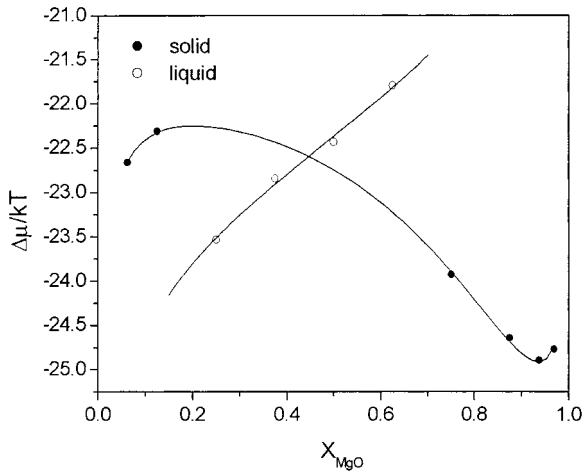

Figure 2. Chemical potential vs composition at $T = 2500$ K. (●) Solid phase. (○) Liquid.

Calculation of the Phase Diagram

Given the dependence of the chemical potential difference $\Delta\mu = \mu_{Ca} - \mu_{Mg}$ on concentration, the thermodynamic potential and hence the phase diagram of the system can be determined. In practice, this problem is more complicated here than in our earlier work on solid solutions[6] due to the existence of the liquid phase. At temperatures where solid and liquid phases coexist, a plot of $\Delta\mu(x_{Mg})$ vs x_{Mg} contains regions corresponding to solid and to liquid, depending on which phase has the lower thermodynamic potential at any given concentration, as illustrated in Figure 2. To extract the phase diagram from the simulations, it is necessary to find the thermodynamic potential for *both* phases. The coexistence concentrations can then be found from the usual double tangent construction.

The calculated values of $\Delta\mu(x_{Mg})$ were fitted to a cubic polynomial in x_{Mg} similar in form to that used in the Margules approximation for solid solutions:[25]

$$\frac{\Delta\mu_{s(l)}}{kT} = \ln\frac{x}{1-x} + a_{s(l)} + b_{s(l)}x + c_{s(l)}x^2 + d_{s(l)}x^3 \quad (12)$$

where *s(l)* refers to solid (liquid) phase and we have dropped the Mg subscript for clarity. The cubic term was found to be negligible for the liquid phase, but it is important to keep this term for the solid phase to describe the asymmetry of the calculated $\Delta\mu_s$. Integrating with respect to x_{Mg} gives $G(x_{Mg})$:

$$\frac{G_{s(l)}}{kT} = x\ln x + (1-x)\ln(1-x) + a_{s(l)}x + \frac{1}{2}b_{s(l)}x^2 + \frac{1}{3}c_{s(l)}x^3 + \frac{1}{4}d_{s(l)}x^4 + C_{s(l)} \quad (13)$$

for both phases. The last unknown parameter for both phases is the constant $C_{s(l)}$, which depends only on temperature; in fact, only the difference between these constants $C_s - C_l$ is required to compare the free energy of solid and liquid phases. When $x_{Mg} = 0$ (pure CaO), then at the melting point, 2600 K, the free energies of both phases are equal and $C_s - C_l = 0$. Similarly, at $T = 2870$ K (the melting point of pure MgO), the free energies of liquid and solid are equal when $x_{Mg} = 1$, from which we can obtain the value of $C_s - C_l$. We assume $C_s - C_l$, which we need only over a 500 K temperature range, varies linearly with

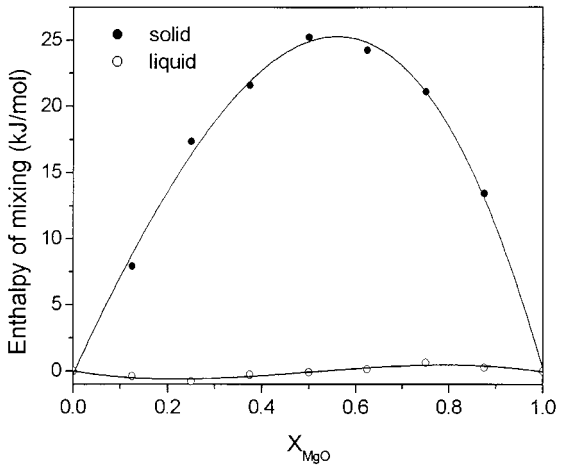

Figure 3. Calculated values of ΔH_{mix} (kJ mol^{-1}) at $T = 2000$ K (solid state, ●) and $T = 3000$ K (liquid state, ○).

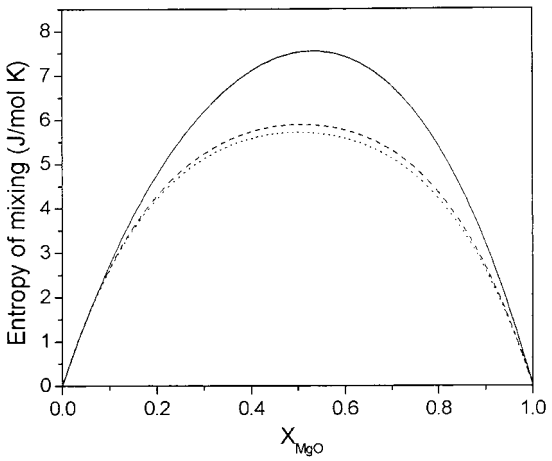

Figure 4. Calculated values of ΔS_{mix} (J mol^{-1} K^{-1}) at $T = 2000$ K (solid state, —) and $T = 3000$ K (liquid state, − −). For comparison, the ideal entropy of mixing is also shown (− −).

T. We have checked this is a good approximation by also extracting the value of $C_s - C_l$ at 2400 K where $\Delta\mu(x_{Mg})$ also shows a jump between solid and liquid phases for $x_{Mg} = 0.26$. We thus have all the data necessary to calculate the phase diagram.

Results

Figure 3 shows the calculated enthalpy of mixing of solid CaO/MgO as a function of composition at $T = 2000$ K and the enthalpy of mixing of liquid CaO/MgO at $T = 3000$ K. The curve for the solid system is somewhat asymmetric, with a maximum of 25.4 kJ mol^{-1} for a mole fraction of MgO of about 0.54. Our results for ΔH_{mix} are substantially lower than those obtained by Ceder and co-workers[10] who used the same set of potentials and, for example, predict enthalpies as high as ≈49 kJ mol^{-1} for a mixture comprising 50% CaO/50% MgO. We attribute this difference to the fact that in ref 10, only ordered cation arrangements in relatively small unit cells (up to 64 ions) are studied. As shown above, in the absence of exchanges the results for ΔH_{mix} in Monte Carlo can be substantially higher, closer to the results by Ceder et al.[10] We have previously evaluated[8,26] enthalpies of mixing in the solid state for *small* CaO concentrations up to $x_{Ca} = 0$ using hybrid Monte Carlo and quasiharmonic lattice dynamics methods. The results obtained here are in good agreement with these previous data. For the liquid system, ΔH_{mix} is close to zero, which indicates almost ideal behavior.

Entropies of mixing can be extracted from the free energies and enthalpies of mixing. Values of ΔS_{mix} at 2000 and 3000 K are shown in Figure 4 together with the ideal entropy of mixing. The excess entropy in the solid state can be as high as 30% of the ideal entropy, which is substantially higher than that of MgO/MnO;[6] like the excess enthalpy, the entropy curve is slightly asymmetric. These results are also in good agreement with those obtained using our configurational lattice dynamics approach to solid solutions;[26] however, these lattice dynamics calculations were restricted to compositions <16% CaO since at higher CaO concentrations the quasiharmonic approximation broke down, preventing full free energy minimization. Although ΔH_{mix} for CaO/MgO is large and positive, it is clear that this is offset in the single-phase regions by large, positive values of ΔS_{mix}, which are in excess of the "ideal" value. In the liquid system ($T =$ 3000 K), ΔS_{mix} is much smaller than in the solid, again indicating that the solution is close to ideal.

The calculated dependence of $\Delta G(x_{Mg})$ at four different temperatures is shown in Figure 5. At $T = 2400$ K the system is solid at all concentrations (Figure 5a): the straight line (common tangent) defining the two phase region does not intersect the dashed line showing the calculated free energy of the liquid phase. At 2440 K (Figure 5b) this common tangent is also a tangent to the liquid-phase curve, and so all three phases coexist at this temperature (the eutectic point). The concentration of Mg in the liquid phase is 0.32. For comparison, the experimental value[22] of $T^{eutectic}$ is 2647 K, at a Mg mole fraction, $x_{MgO}^{eutectic} = 0.41$. At a higher temperature, 2500 K, the liquid-phase coexists with one of the two solid phases, depending on the overall composition of the system (Figure 5c). The highest temperature, 2900 K, (Figure 5d) corresponds to liquid at all compositions.

The resulting phase diagram is shown in Figure 6. The overall agreement with the experimental phase diagram is good. All the characteristic features of the MgO/CaO phase diagram, including the eutectic point and the regions of liquid−solid coexistence, are reproduced. We predict that solid MgO is more soluble in solid CaO than CaO in MgO, in agreement with the experiments of Doman et al.[22] and of Trojer and Konopicky.[27]

Final Remarks

We have shown in this paper how exchange-bias Monte Carlo may be used to calculate the phase diagram of binary oxides for both melt and solid phases. To our knowledge this is the first time this has been achieved for ceramics. The calculated MgO/CaO phase diagram reproduces all the characteristic features of the experimental phase diagram, including the eutectic point and the regions of liquid−solid coexistence. Enthalpies and entropies of mixing are in surprisingly good agreement with those obtained for the solid solution using configurationally averaged lattice dynamics at compositions where such data exist. Our results do not agree with those of ref 10 obtained using different techniques. A major advantage of our exchange-bias Monte Carlo approach over lattice dynamics and CVM is that it is also applicable to the liquid phase.

The key feature of our method which is applicable to any composition is that it samples many configurations, explicitly considering different arrangements of ions, and allows for the *local* structural relaxation surrounding each cation. This relaxation is crucial. If ignored, the energy of exchange of any two ions is usually very high and all exchanges are rejected, thus sampling only one arrangement. Vibrational effects are included and the method can be used at any pressure and temperature. Work is currently in progress to develop the

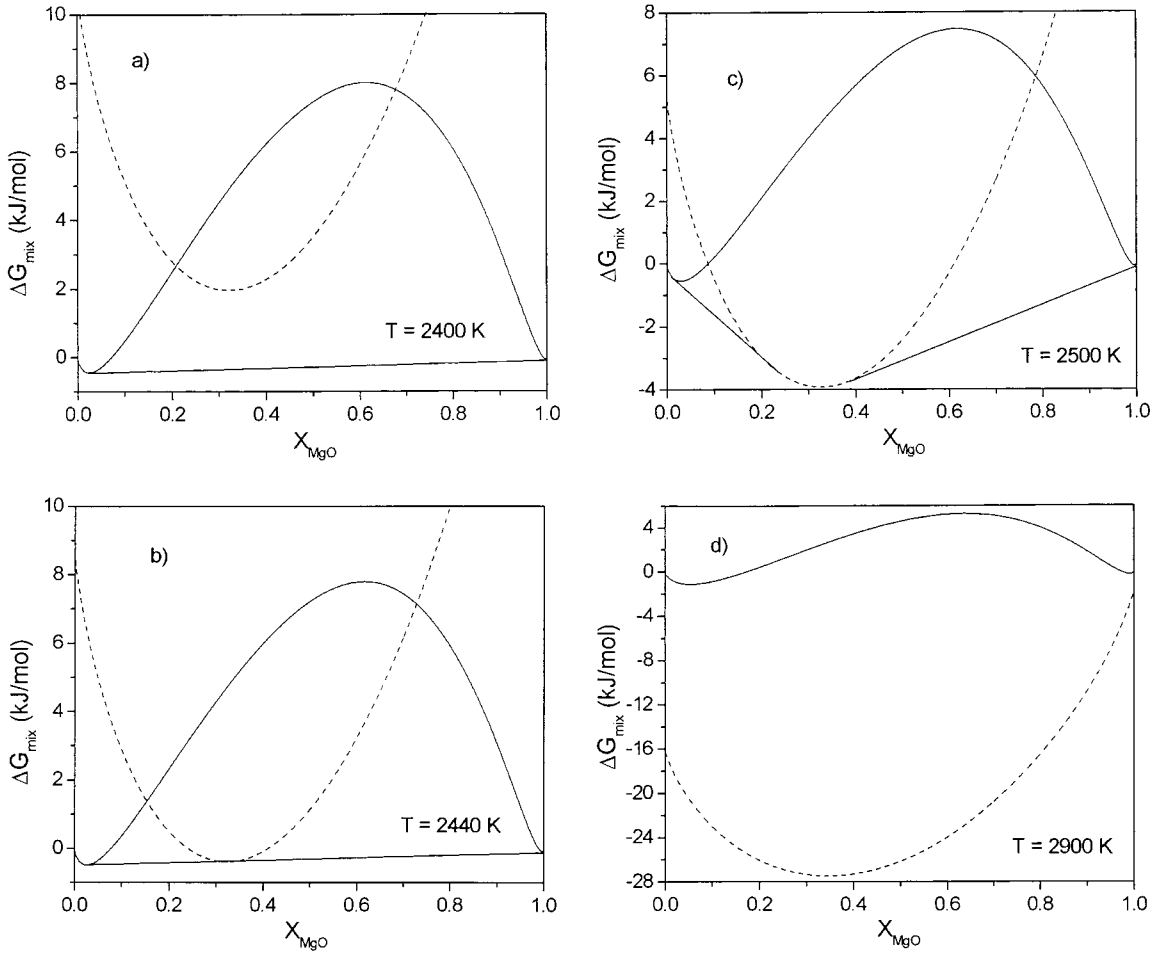

Figure 5. ΔG_{mix} vs composition at (a) $T = 2400$ K, (b) $T = 2440$ K, (c) $T = 2500$ K, (d) $T = 2900$ K. (—) Solid phase. (– –) Liquid phase.

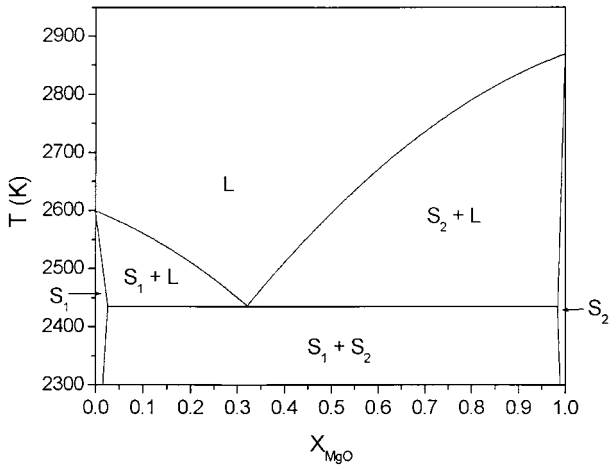

Figure 6. Calculated phase diagram of CaO/MgO. S_1 denotes solution of MgO in solid CaO, S_2 solution of CaO in solid MgO, L corresponds to the liquid mixture of both components. S_1+L, S_2+L, and $S_1 + S_2$ are regions of coexistence of corresponding phases.

methods further, e.g., to ternary mixtures and solid solutions involving heterovalent cations, and to apply them to more complex systems.

Acknowledgment. This work was funded by EPSRC grants GR/M34799, GR/M53899 and ANPCyT grant BID 802/OC-AR-PICT0361. G.D.B. acknowledges support from el Consejo Nacional de Investigaciones Científicas y Técnicas de la República Argentina, and his contribution to this work has been possible due to a grant from the Fundación Antorchas.

References and Notes

(1) de Fontaine, D. *Solid State Phys.* **1994**, *47*, 33.

(2) For example, see: Catlow, C. R. A.; Mackrodt, W. C. *Computer Simulation of Solids*; Catlow, C. R. A., Mackrodt, W. C. Eds.; Springer-Verlag: Berlin; 1982; Chapter 1.

(3) For example, see: Taylor, M. B.; Barrera, G. D.; Allan, N. L.; Barron, T. H. K.; Mackrodt, W. C. *Faraday Discuss.* **1997**, *106*, 377.

(4) Purton, J. A.; Blundy J. D.; Taylor, M. B.; Barrera, G. D.; Allan, N. L. *Chem. Commun.* **1998**, 627.

(5) Allan, N. L.; Barrera, G. D.; Fracchia, R. M.; Lavrentiev, M. Yu.; Taylor, M. B.; Todorov, I. T.; Purton, J. A. *Phys. Rev.* **2001**, *63*, 094203.

(6) Allan, N. L.; Barrera, G. D.; Lavrentiev, M. Yu.; Todorov, I. T.; Purton, J. A. *J. Mater. Chem.* **2001**, *11*, 63.

(7) Shannon, R. D. *Acta Crystallogr., Sect A* **1976**, *32*, 751.

(8) Allan, N. L.; Barrera, G. D.; Purton, J. A.; Sims, C. E.; Taylor, M. B. *Phys. Chem., Chem. Phys.* **2000**, *2*, 1099.

(9) Lewis, G. V.; Catlow, C. R. A. *J. Phys. C: Solid State Phys.* **1985**, *18*, 1149.

(10) Tepesh, P. D.; Kohan, A. F.; Garbulsky, G. D.; Ceder, G.; Coley, C.; Stokes, H. T.; Boyer, L. L.; Mehl, M. J.; Burton, B. P.; Cho, K.; Joannopoulos, J. *J. Am. Ceram. Soc.* **1996**, *79*, 2033; Kohan, A. F.; Ceder, G. *Phys. Rev. B* **1996**, *54*, 805.

(11) Metropolis, N. I.; Rosenbluth, A. W.; Rosenbluth, M. N.; Teller, A. H.; Teller, E. *J. Chem. Phys.* **1953**, *21*, 1087.

(12) Frenkel, D.; Smit, B. *Understanding Molecular Simulation*; Academic Press: San Diego, 1996.

(13) Purton, J. A.; Barrera, G. D.; Allan, N. L.; Blundy, J. D. *J. Phys. Chem. B* **1998**, *102*, 5202.

(14) Eppinga, P.; Frenkel, D. *Mol. Phys.* **1984**, *52*, 1303.

(15) Kofke, D. A.; Glandt, E. D. *Mol. Phys.* **1988**, *64*, 1105.

(16) Smolander, K. J. *Phys. Scr.* **1990**, *42*, 485.

(17) Matsui, M.; Price, G. D. *Nature* **1991**, *351*, 735.

(18) Kapusta, B.; Guillope, M. *Phys. Earth Planet. Inter.* **1993**, *75*, 205.

(19) Kubicki, J. D.; Lasaga, A. C. *Am. J. Science* **1992**, *292*, 153.

(20) Belonoshko, A. B. *Geochim. Cosmochim. Acta* **1994**, *58*, 4039.

(21) Belonoshko, A. B.; Dubrovinsky, L. S. *Am. Mineral.* **1996**, *81*, 303.

(22) Doman, R. C.; Barr, J. B.; McNally, R. N.; Alper, A. M. *J. Am. Ceram. Soc*. **1963**, *46*, 313.
(23) *Concise Encyclopedia of Chemistry*; Walter de Gruyter: New York, 1994.
(24) *Lange's Handbook of Chemistry*; McGraw-Hill: New York, 1985.
(25) e.g., Thompson, J. B. *Researches in Geochemistry*, Abelson, P. H., Ed.; John Wiley: New York, 1967; Vol. II, p 340.
(26) Fracchia, R. M.; Purton, J. A.; Allan, N. L.; Barron, T. H. K.; Barrera. G. D.; Blundy, J. D. *Radiat. Eff. Defects Solids* **1999**, *151*, 197.
(27) Trojer, F.; Konopicky, K. *Radex Rundsch*. **1949**, *4*, 16.